

Electronic Supplementary Information

Dye-catalyst dyads for photoelectrochemical water oxidation based on metal-free sensitizers

Cristina Decavoli,^a Chiara L. Boldrini,^a Vanira Trifiletti,^b Sally Luong,^b Oliver Fenwick,^b Norberto Manfredi,^{*a} and Alessandro Abbotto^{*a}

^a Department of Materials Science and INSTM Unit, Solar Energy Research Center MIB-SOLAR, University of Milano – Bicocca, Via R. Cozzi 55, I-20125, Milano, Italy

^b School of Engineering and Materials Science (SEMS), Queen Mary University of London, Mile End Road, London E1 4NS, UK

Email: alessandro.abbotto@unimib.it; norberto.manfredi@unimib.it

Table of Content

Figure S1. Absorption spectra of 1- μm TiO_2 film sensitized by the investigated dyes (solid line) and corresponding dyads (dash-dot line).....	4
Figure S2. CV of dyes in solution in TBAClO_4 0.1 M in DMF degassed with Ar.....	4
Figure S3. DPV of dyes in solution in TBAClO_4 0.1 M in DMF degassed with Ar.	5
Figure S4. CV of dye CBZ-4Py, corresponding dyad CBZ-4Py+Ru, and of the Ru-precursor (Ru) on a 3- μm -thick TiO_2 film (0.196 cm^2) in TBAClO_4 0.1 M in CH_3CN degassed with Ar.	5
Figure S5. CV of dye CBZ-3Py, corresponding dyad CBZ-3Py+Ru, and of the Ru-precursor (Ru) on a 3- μm -thick TiO_2 film (0.196 cm^2) in TBAClO_4 0.1 M in CH_3CN degassed with Ar.	6
Figure S6. CV of CBZ-4Py, CBZ-4Py+Ru and corresponding N-alkylcarbazole (CBZ-Th) on 3.5- μm -thick TiO_2 film in TBAClO_4 0.1 M in CH_3CN degassed with Ar.....	6
Figure S7. XPS survey spectra of the investigated dyes and dyads compared to the TiO_2 spectrum; core-levels involved in the bonding interaction between TiO_2 and the dyes are labelled in red.....	7
Figure S8. XPS spectra of the high-resolution core level for N 1s region of the investigated dyes and dyads compared to the bare TiO_2	7
Figure S9. XPS valence-level spectrum of the investigated dyes and dyads compared to the bare TiO_2 ; in the inset, the enlargement of the spectrum in the region where the contribution of ruthenium is clearly visible below 3.5 eV.	8
Figure S10. Linear sweep voltammogram (LSV) of TiO_2 films sensitized with CBZ-4Py+Ru (red) and CBZ-3Py+Ru (black) in 0.1 M Na_2SO_4 at pH 5.8 under chopped illumination (200 W Xe lamp; $420 < \lambda < 800$ nm).....	8
Figure S11. Chronoamperometry of TiO_2 films sensitized with CBZ-3Py (red) and CBZ-3Py+Ru (black) in 0.1 M Na_2SO_4 at pH 5.8 with an applied bias of ~ 0.5 V vs NHE under illumination (200 W Xe lamp; $420 < \lambda < 800$ nm).....	9
Figure S12. Chronoamperometry of TiO_2 films sensitized with CBZ-4Py (red) and CBZ-4Py+Ru (black) in 0.1 M Na_2SO_4 at pH 5.8 with an applied bias of ~ 0.5 V vs NHE under illumination (200 W Xe lamp; $420 < \lambda < 800$ nm).....	9
Figure S13. 2-hours-chronoamperometry of TiO_2 films sensitized with CBZ-3Py+Ru in 0.1 M Na_2SO_4 at pH 5.8 with an applied bias of ~ 0.5 V vs NHE under illumination (200 W Xe lamp; $420 < \lambda < 800$ nm).....	10
Figure S14. 2-hours-chronoamperometry of TiO_2 films sensitized with CBZ-4Py+Ru in 0.1 M Na_2SO_4 at pH 5.8 with an applied bias of ~ 0.5 V vs NHE under illumination (200 W Xe lamp; $420 < \lambda < 800$ nm).....	10
Figure S15. Collector-Generator plot of a CBZ-4Py+Ru sensitized electrode. Black line: current–time trace at illuminated (200 W Xe lamp; $420 < \lambda < 800$ nm) CBZ-4Py+Ru dyad on TiO_2 in 0.1 M Na_2SO_4 at pH 5.8 with an applied bias of ~ 0.5 V vs NHE. Red line: current–time traces at an FTO collector electrode, 300 μm from the photoanode at an applied bias of ~ -0.6 V vs NHE measured concurrently with the photoelectrochemical–time trace (FE of shown measurement = 65%).....	11

Figure S16. Incident photon-to-current efficiency (IPCE) of TiO₂ films sensitized with CBZ-3Py (black) and CBZ-3Py+Ru (red) in 0.1 M Na₂SO₄ at pH 5.8 with an applied bias of ~0.5 V vs NHE under monochromatic illumination.	11
Figure S17. Incident photon to current efficiency of TiO₂ films sensitized with CBZ-4Py (black) and CBZ-4Py+Ru (red) in 0.1 M Na₂SO₄ at pH 5.8 with an applied bias of ~0.5 V vs NHE under monochromatic illumination.....	12
Figure S18. Light harvesting efficiency (LHE) of TiO₂ films sensitized with the investigated dyads.	12
Figure S19. Absorbed photon-to-current efficiency (APCE) of TiO₂ films sensitized with the investigated dyads.....	13
<i>¹H and ¹³C NMR</i>.....	14
Figure S20. ¹H NMR of 2 in CDCl₃.....	14
Figure S21. ¹H NMR of 3a in CDCl₃.....	14
Figure S22. ¹H NMR of 3b in CDCl₃.....	15
Figure S23. ¹H NMR of 4a in DMSO-d₆.....	15
Figure S24. ¹H NMR of 4b in DMSO-d₆.....	16
Figure S25. ¹H NMR of CBZ-4Py in DMSO-d₆.....	16
Figure S26. ¹³C NMR of CBZ-4Py in DMSO-d₆.....	17
Figure S27. ¹H NMR of CBZ-3Py in DMSO-d₆.....	17
Figure S28. ¹³C NMR of CBZ-3Py in DMSO-d₆.....	18
<i>IR spectra</i>.....	19
Figure S29: FT-IR spectrum of CBZ-4Py.....	19
Figure S30: FT-IR spectrum of CBZ-3Py.....	19
<i>HRMS spectra</i>.....	20
Figure S31. HRMS spectrum of CBZ-4Py.....	20
Figure S32. HRMS spectrum of CBZ-3Py.....	20

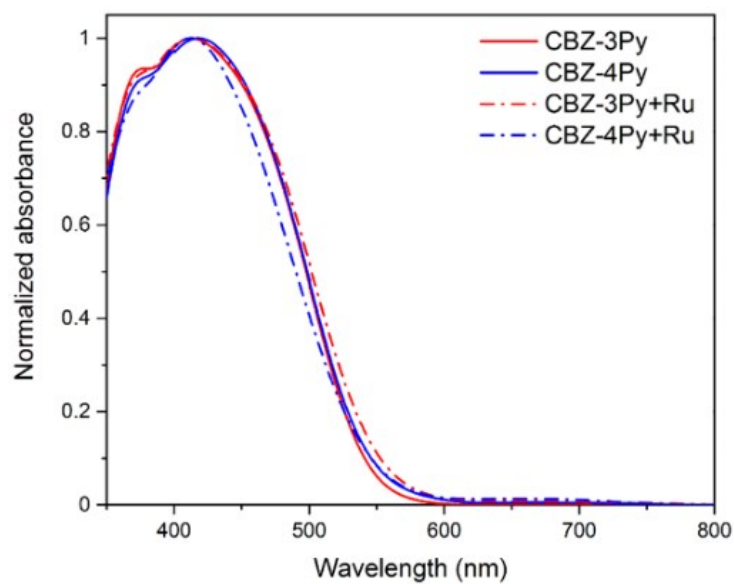


Figure S1. Absorption spectra of 1- μm TiO_2 film sensitized by the investigated dyes (solid line) and corresponding dyads (dash-dot line).

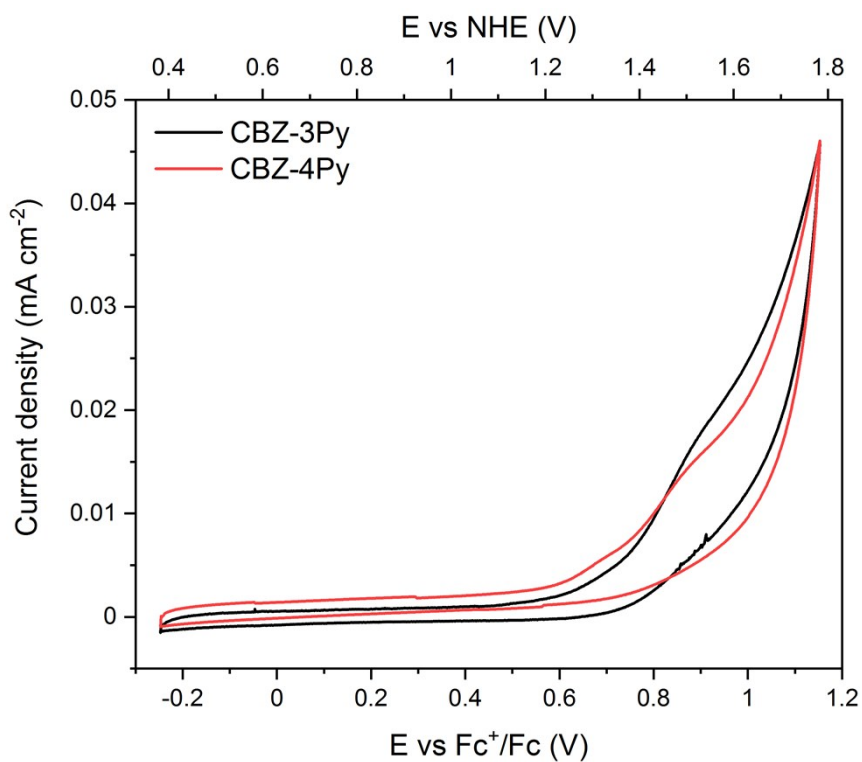


Figure S2. CV of dyes in solution in TBAClO_4 0.1 M in DMF degassed with Ar.

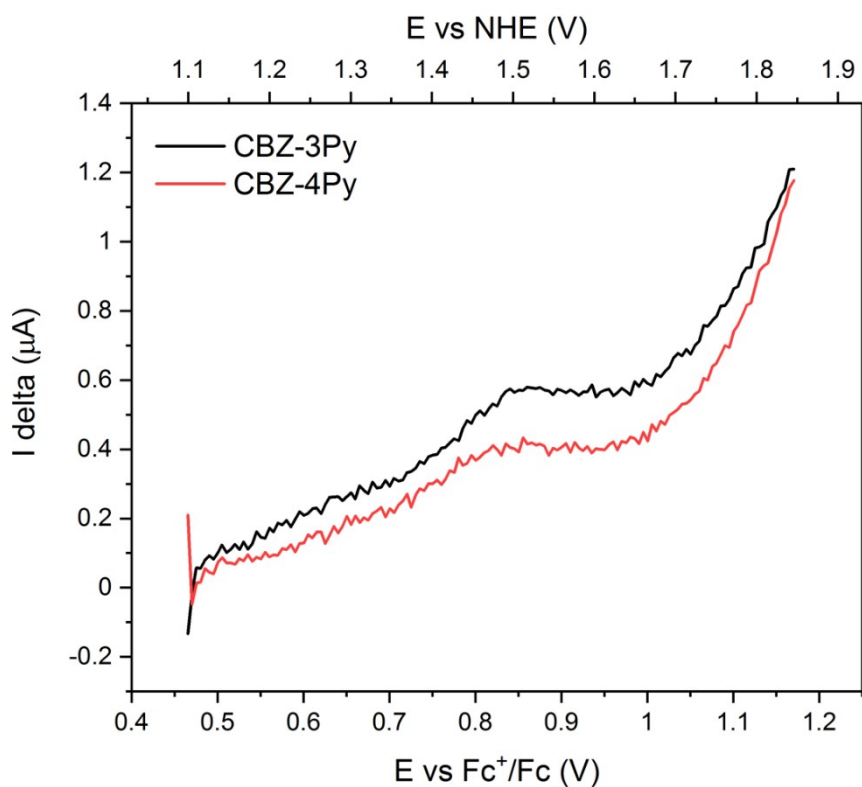


Figure S3. DPV of dyes in solution in TBAClO₄ 0.1 M in DMF degassed with Ar.

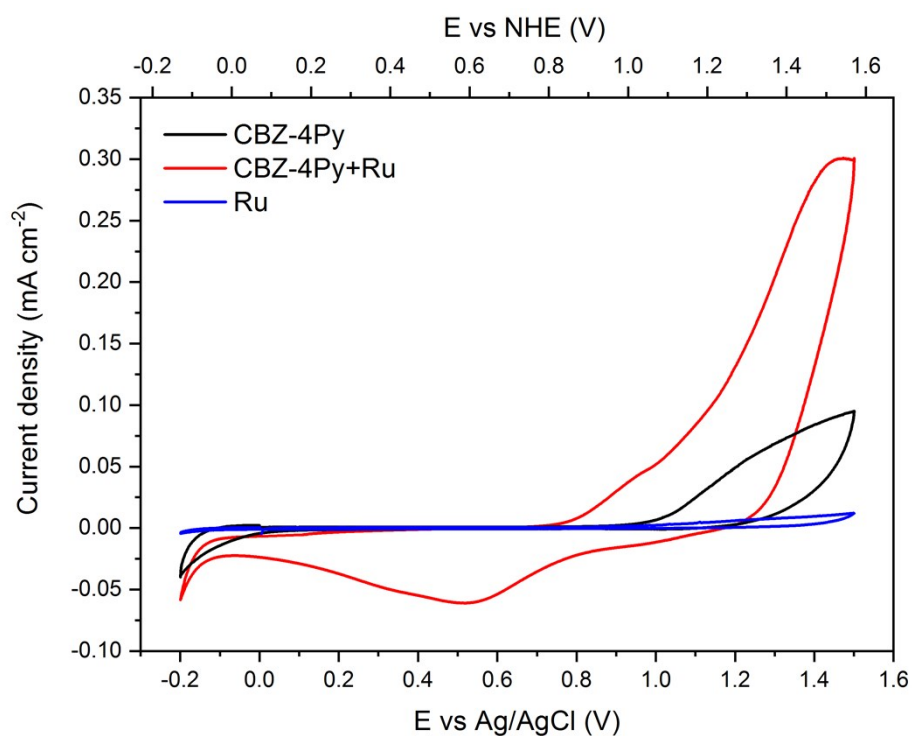


Figure S4. CV of dye **CBZ-4Py**, corresponding dyad **CBZ-4Py+Ru**, and of the Ru-precursor (**Ru**) on a 3- μ m-thick TiO₂ film (0.196 cm²) in TBAClO₄ 0.1 M in CH₃CN degassed with Ar.

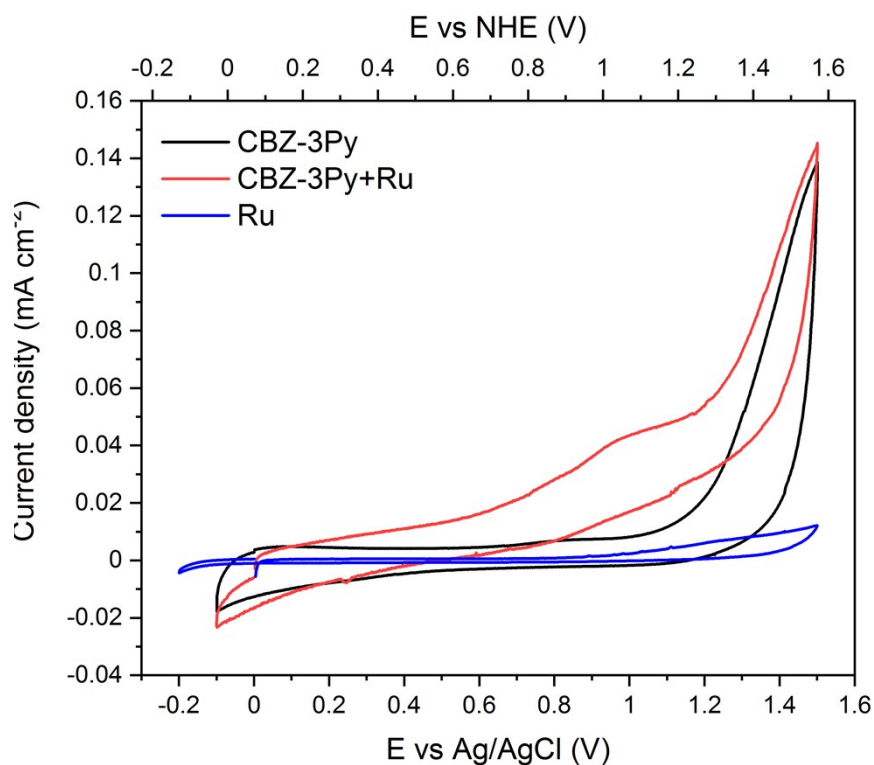


Figure S5. CV of dye **CBZ-3Py**, corresponding dyad **CBZ-3Py+Ru**, and of the Ru-precursor (**Ru**) on a 3- μm -thick TiO_2 film (0.196 cm^2) in TBAClO_4 0.1 M in CH_3CN degassed with Ar.

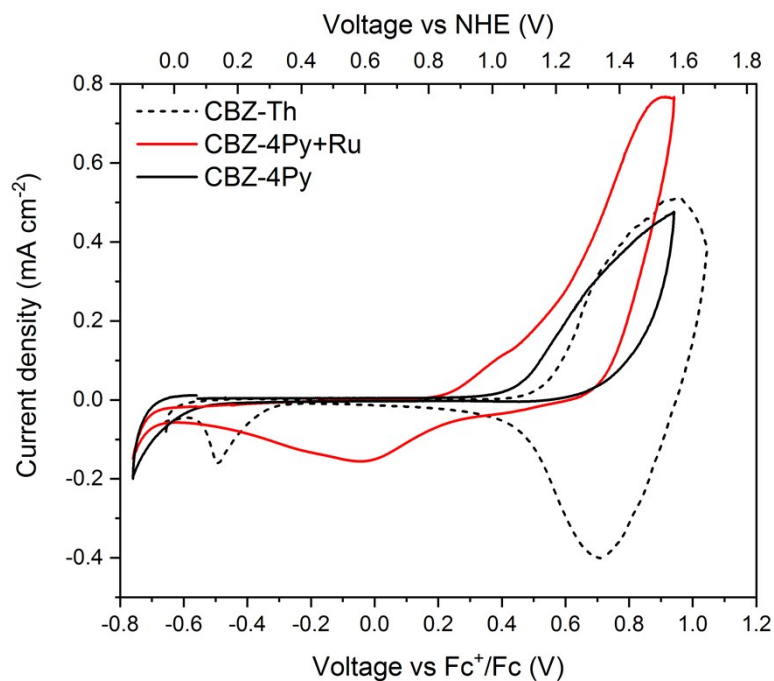


Figure S6. CV of **CBZ-4Py**, **CBZ-4Py+Ru** and corresponding *N*-alkylcarbazole (**CBZ-Th**) on 3.5- μm -thick TiO_2 film in TBAClO_4 0.1 M in CH_3CN degassed with Ar.

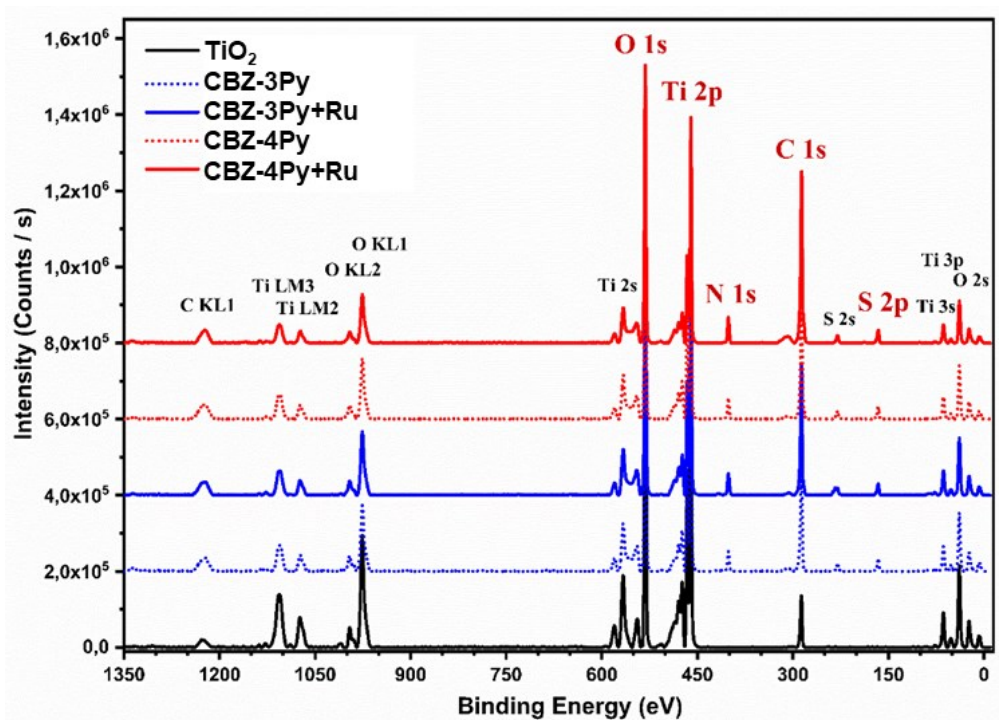


Figure S7. XPS survey spectra of the investigated dyes and dyads compared to the TiO_2 spectrum; core-levels involved in the bonding interaction between TiO_2 and the dyes are labelled in red.

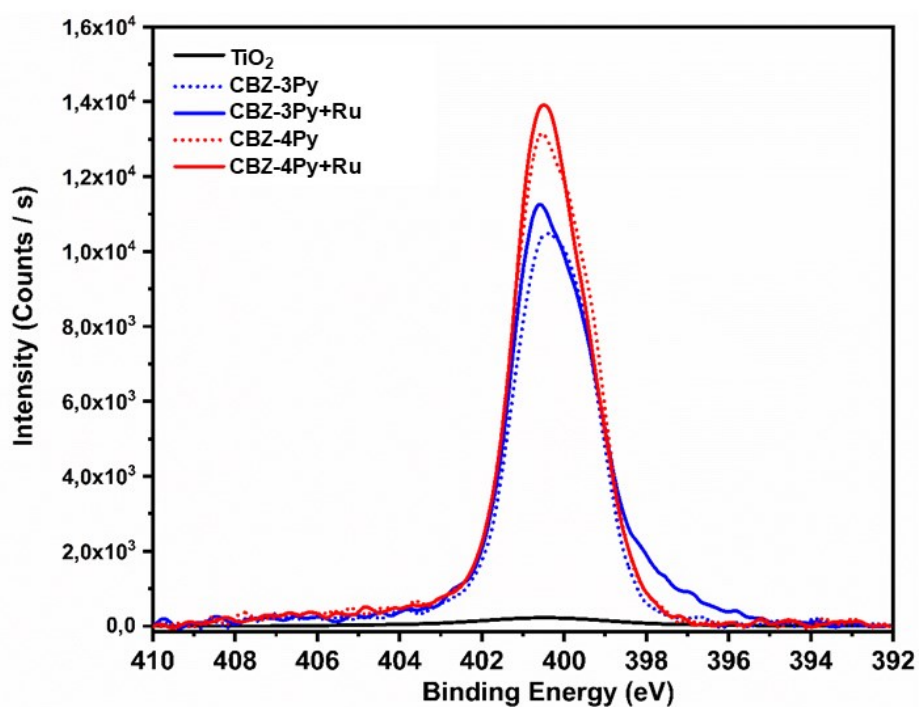


Figure S8. XPS spectra of the high-resolution core level for N 1s region of the investigated dyes and dyads compared to the bare TiO_2 .

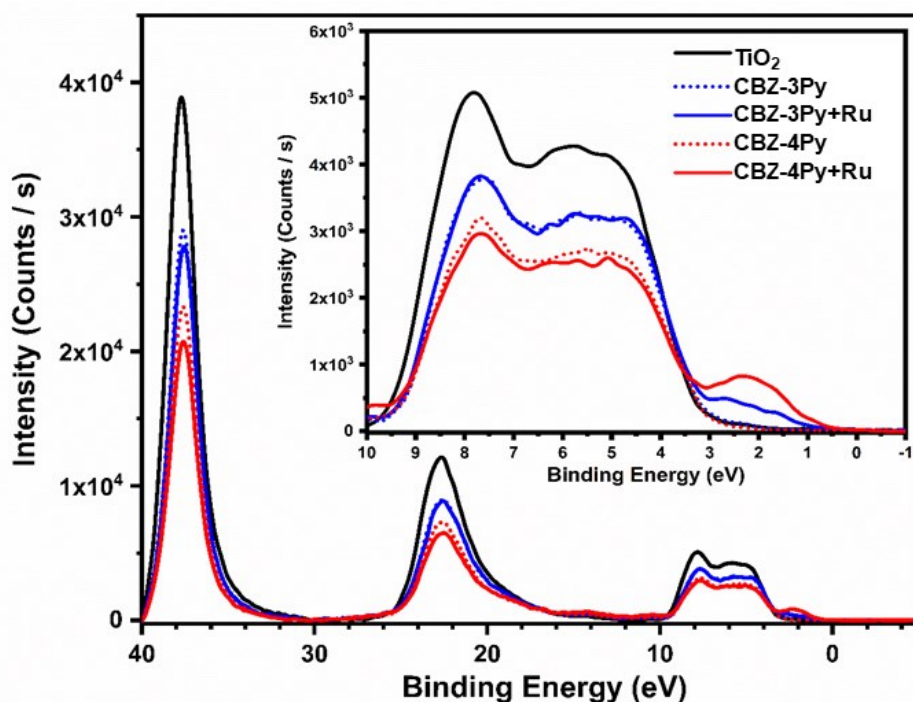


Figure S9. XPS valence-level spectrum of the investigated dyes and dyads compared to the bare TiO_2 ; in the inset, the enlargement of the spectrum in the region where the contribution of ruthenium is clearly visible below 3.5 eV.

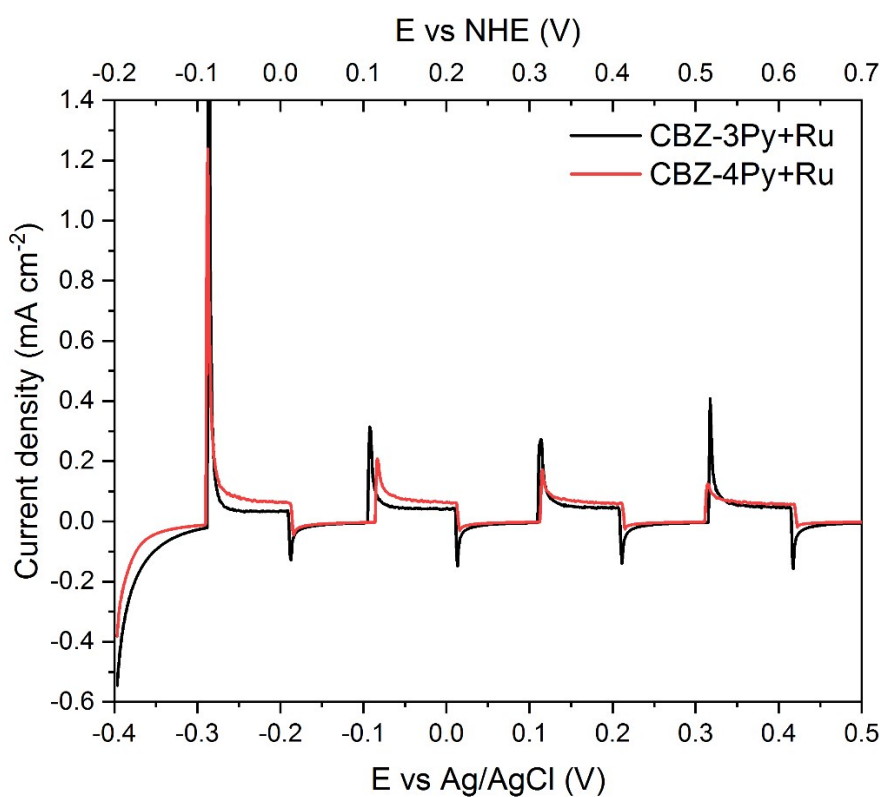


Figure S10. Linear sweep voltammogram (LSV) of TiO_2 films sensitized with **CBZ-4Py+Ru** (red) and **CBZ-3Py+Ru** (black) in 0.1 M Na_2SO_4 at pH 5.8 under chopped illumination (200 W Xe lamp; $420 < \lambda < 800$ nm)

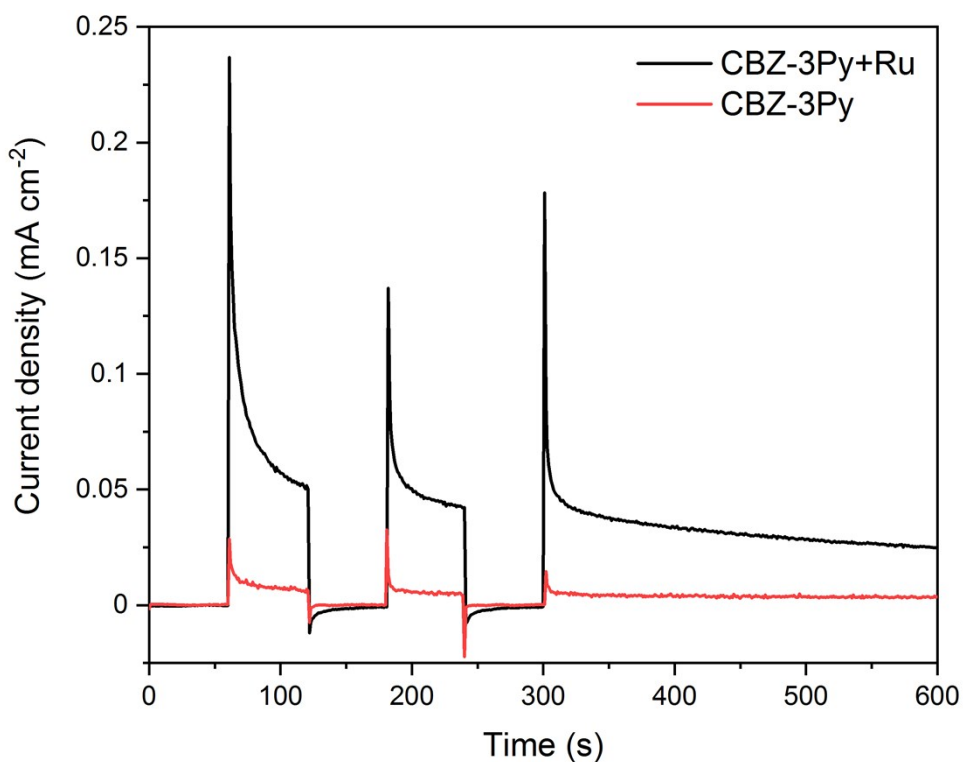


Figure S11. Chronoamperometry of TiO_2 films sensitized with **CBZ-3Py** (red) and **CBZ-3Py+Ru** (black) in 0.1 M Na_2SO_4 at pH 5.8 with an applied bias of ~ 0.5 V vs NHE under illumination (200 W Xe lamp; $420 < \lambda < 800$ nm).

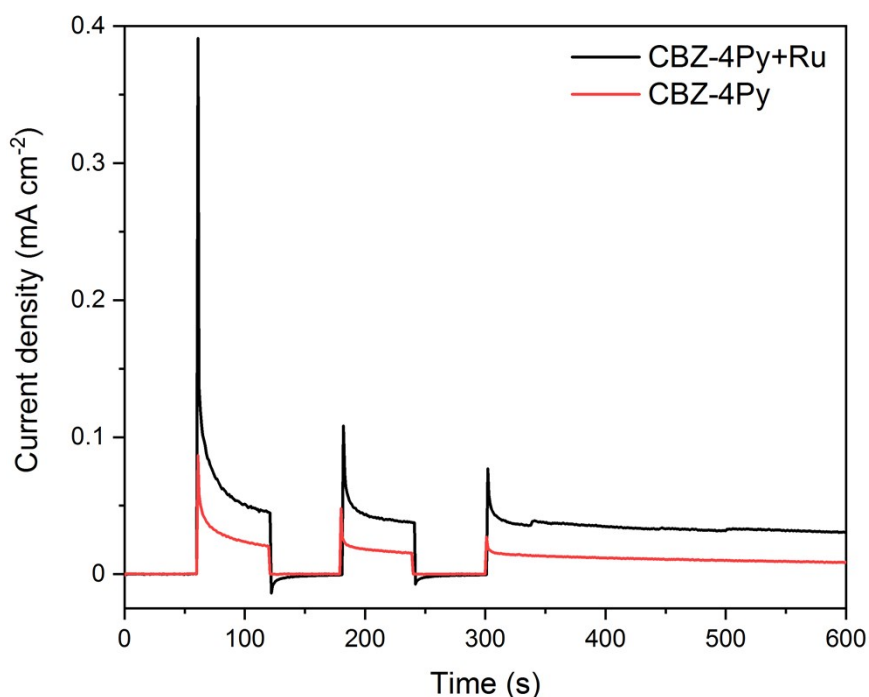


Figure S12. Chronoamperometry of TiO_2 films sensitized with **CBZ-4Py** (red) and **CBZ-4Py+Ru** (black) in 0.1 M Na_2SO_4 at pH 5.8 with an applied bias of ~ 0.5 V vs NHE under illumination (200 W Xe lamp; $420 < \lambda < 800$ nm).

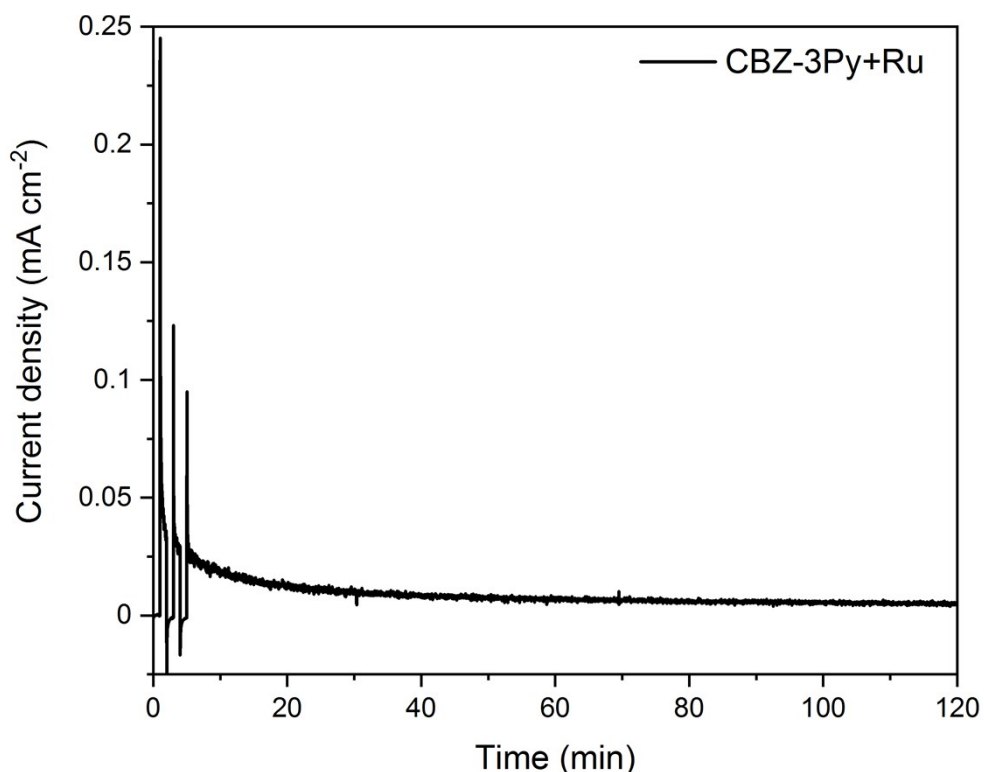


Figure S13. 2-hours-chronoamperometry of TiO_2 films sensitized with **CBZ-3Py+Ru** in 0.1 M Na_2SO_4 at pH 5.8 with an applied bias of ~ 0.5 V vs NHE under illumination (200 W Xe lamp; $420 < \lambda < 800$ nm).

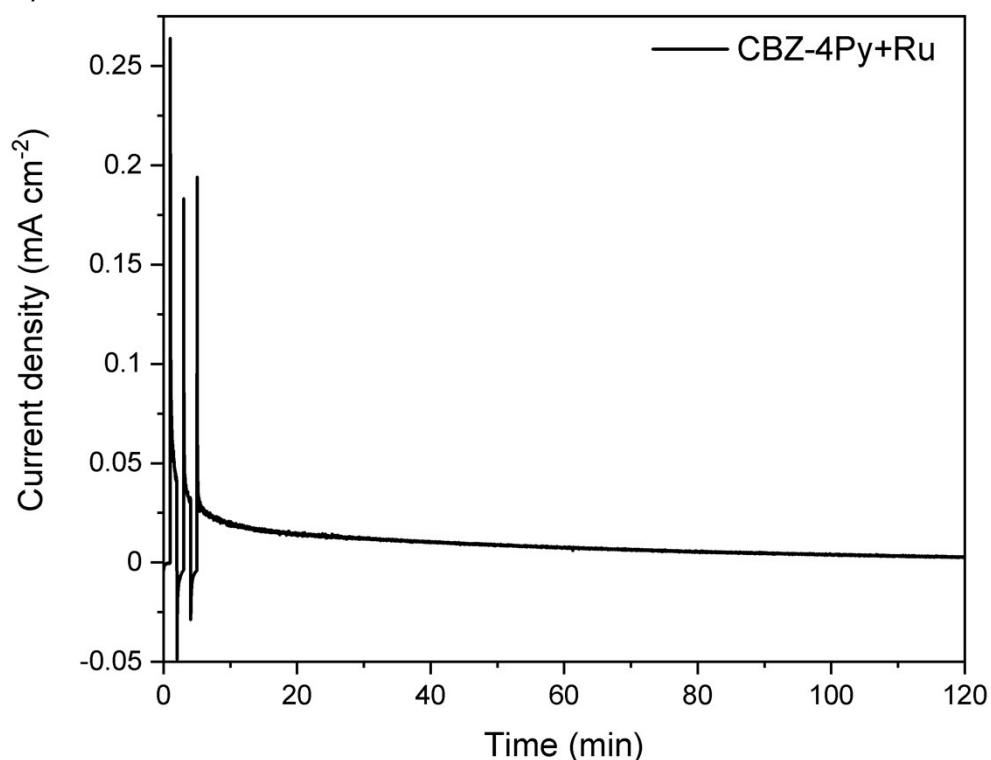


Figure S14. 2-hours-chronoamperometry of TiO_2 films sensitized with **CBZ-4Py+Ru** in 0.1 M Na_2SO_4 at pH 5.8 with an applied bias of ~ 0.5 V vs NHE under illumination (200 W Xe lamp; $420 < \lambda < 800$ nm).

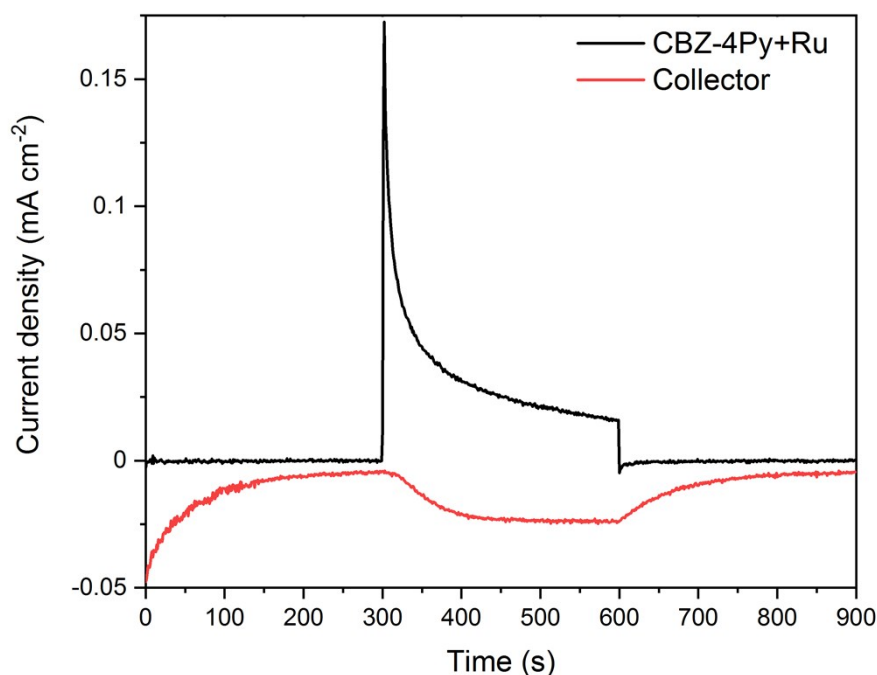


Figure S15. Collector-Generator plot of a **CBZ-4Py+Ru** sensitized electrode. Black line: current–time trace at illuminated (200 W Xe lamp; $420 < \lambda < 800$ nm) **CBZ-4Py+Ru** dyad on TiO_2 in 0.1 M Na_2SO_4 at pH 5.8 with an applied bias of ~ 0.5 V vs NHE. Red line: current–time traces at an FTO collector electrode, 300 μm from the photoanode at an applied bias of ~ -0.6 V vs NHE measured concurrently with the photoelectrochemical–time trace (FE of shown measurement = 65%).

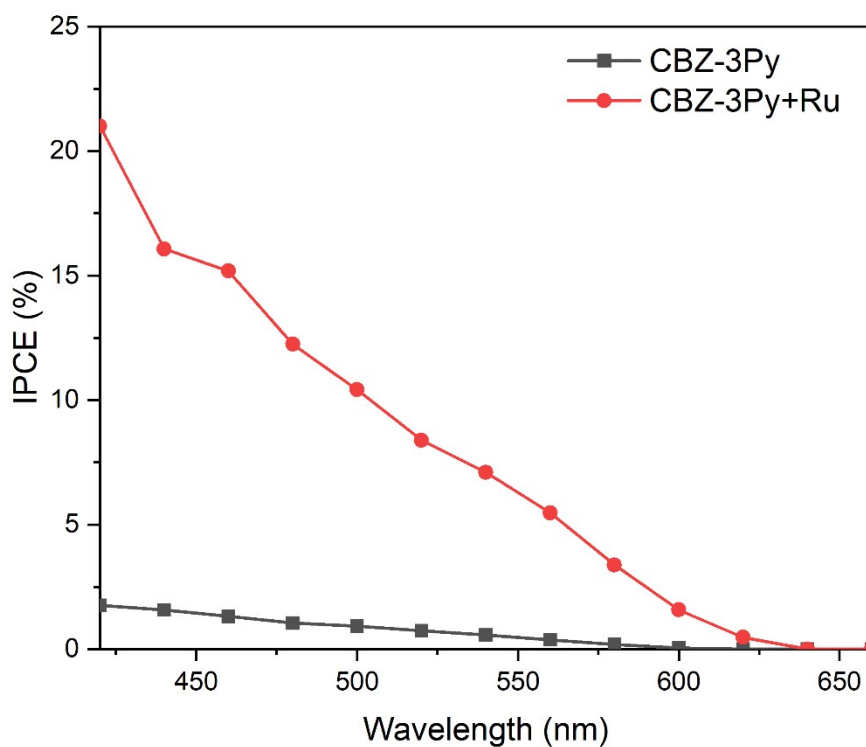


Figure S16. Incident photon-to-current efficiency (IPCE) of TiO_2 films sensitized with **CBZ-3Py** (black) and **CBZ-3Py+Ru** (red) in 0.1 M Na_2SO_4 at pH 5.8 with an applied bias of ~ 0.5 V vs NHE under monochromatic illumination.

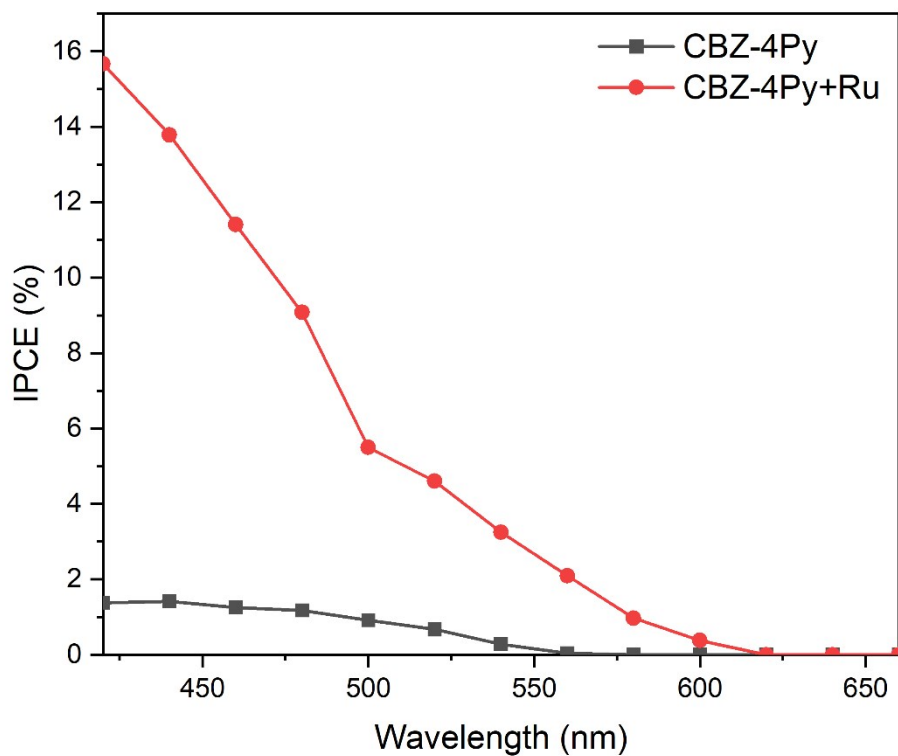


Figure S17. Incident photon to current efficiency of TiO_2 films sensitized with **CBZ-4Py** (black) and **CBZ-4Py+Ru** (red) in 0.1 M Na_2SO_4 at pH 5.8 with an applied bias of ~ 0.5 V vs NHE under monochromatic illumination.

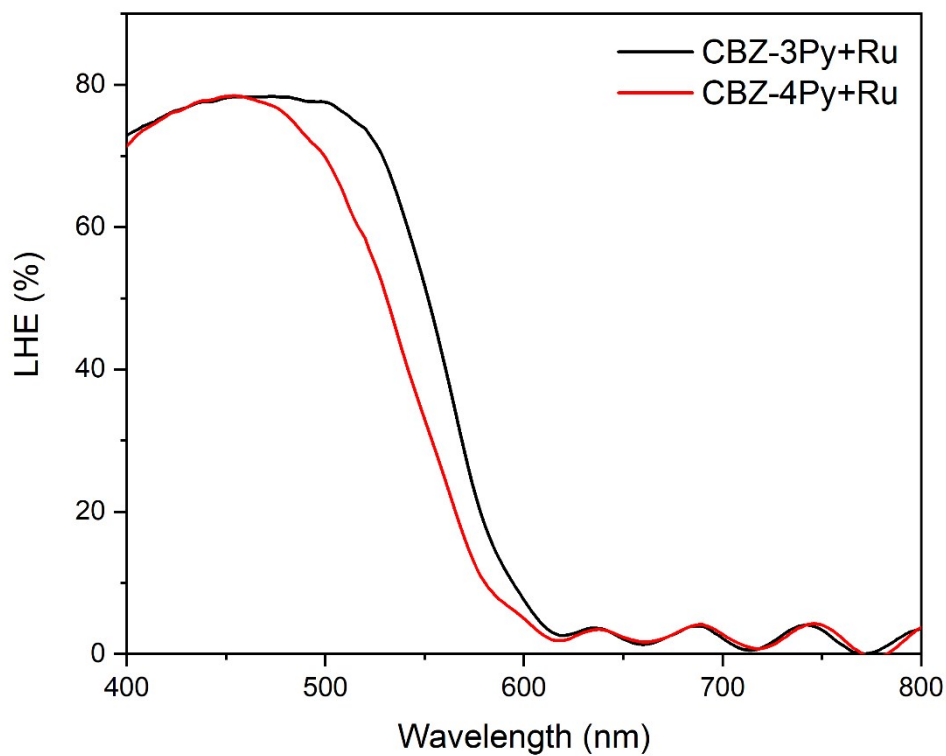


Figure S18. Light harvesting efficiency (LHE) of TiO_2 films sensitized with the investigated dyads.

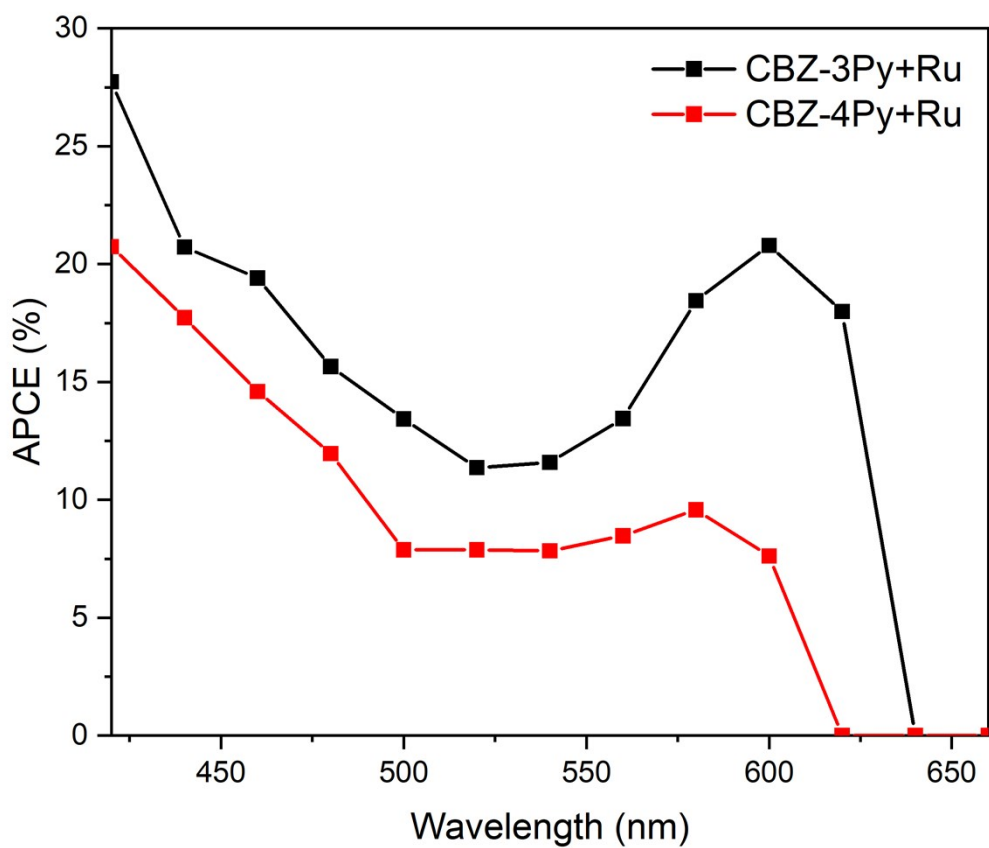


Figure S19. Absorbed photon-to-current efficiency (APCE) of TiO_2 films sensitized with the investigated dyads.

¹H and ¹³C NMR

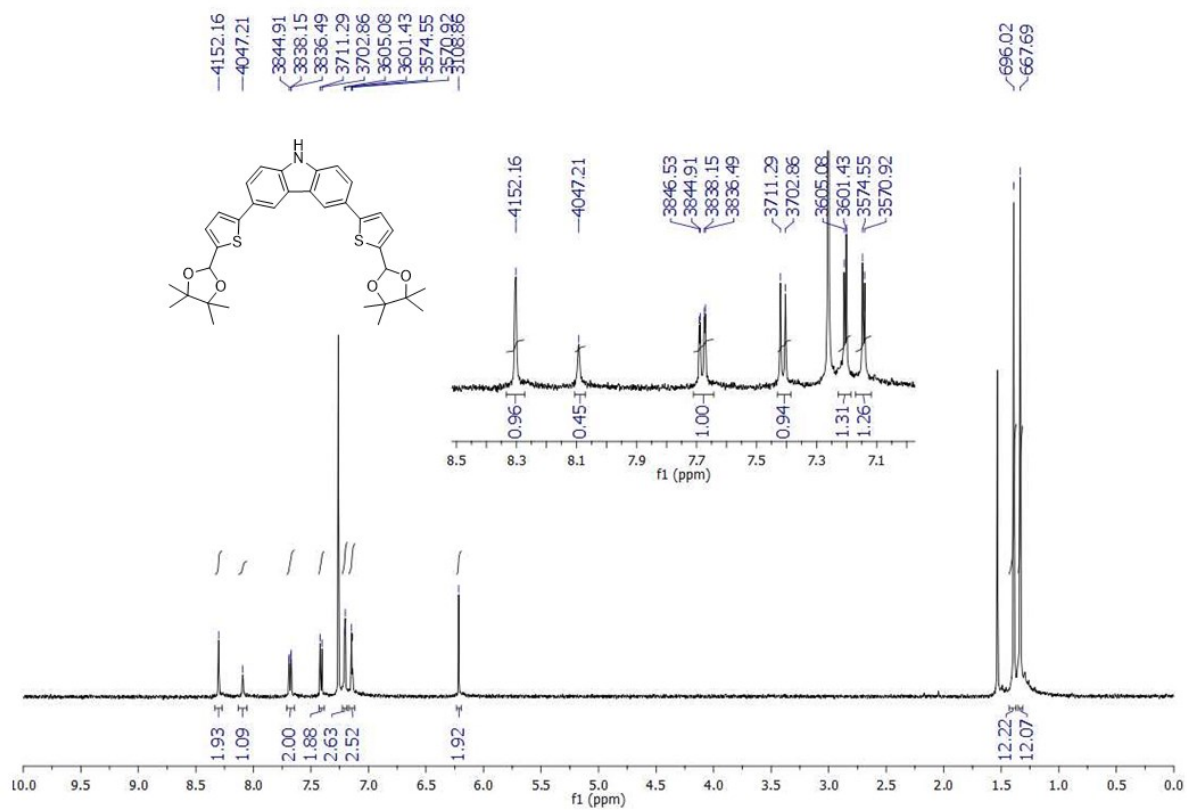


Figure S20. ¹H NMR of **2** in CDCl₃.

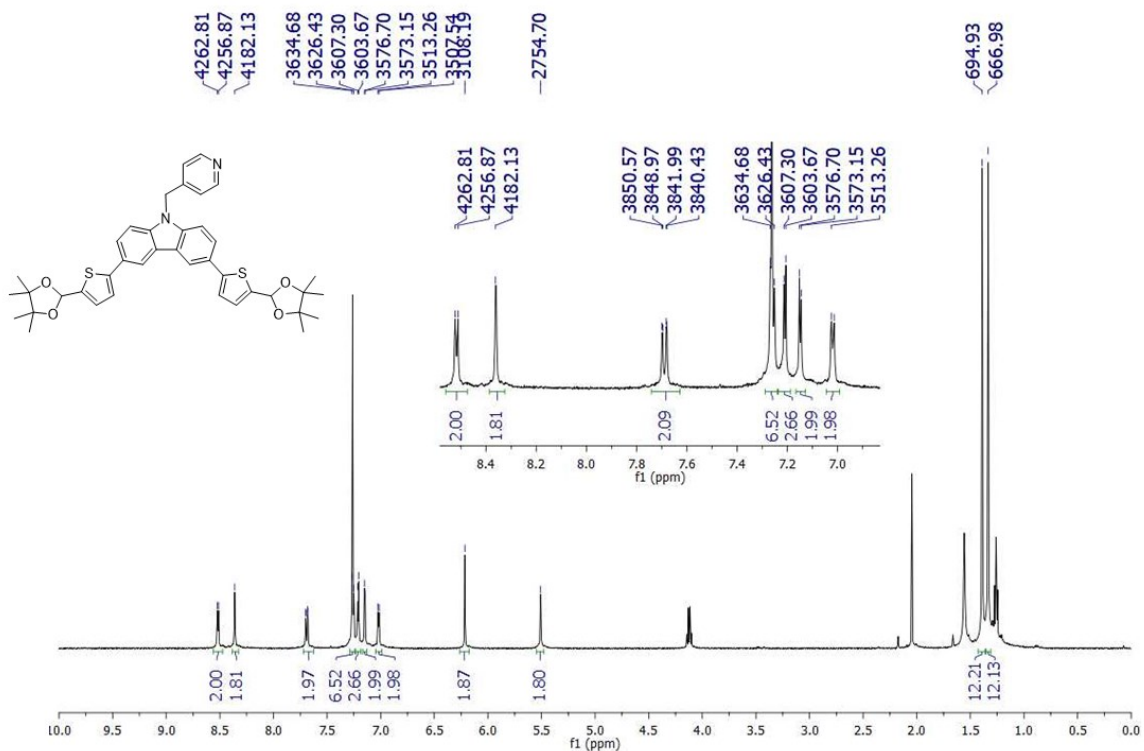


Figure S21. ¹H NMR of **3a** in CDCl₃.

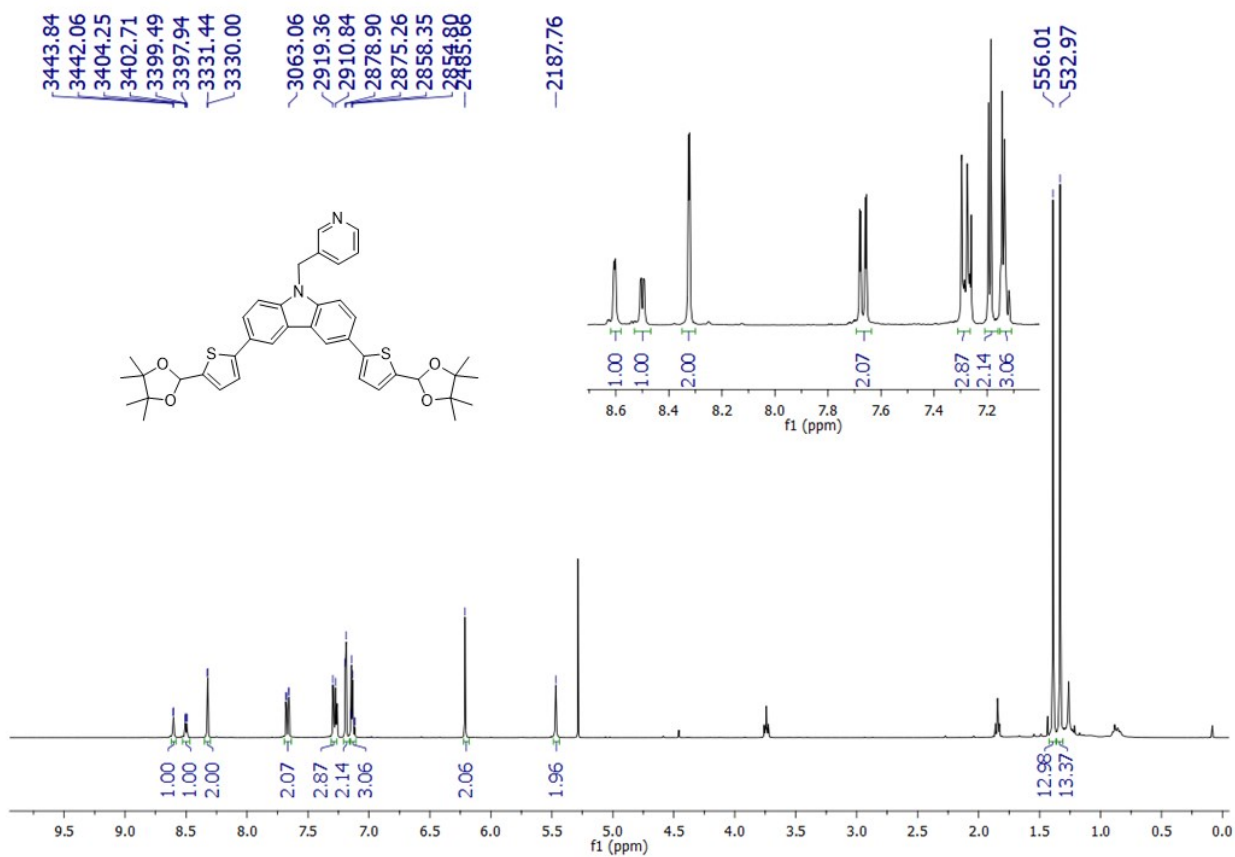


Figure S22. $^1\text{H NMR}$ of **3b** in CDCl_3 .

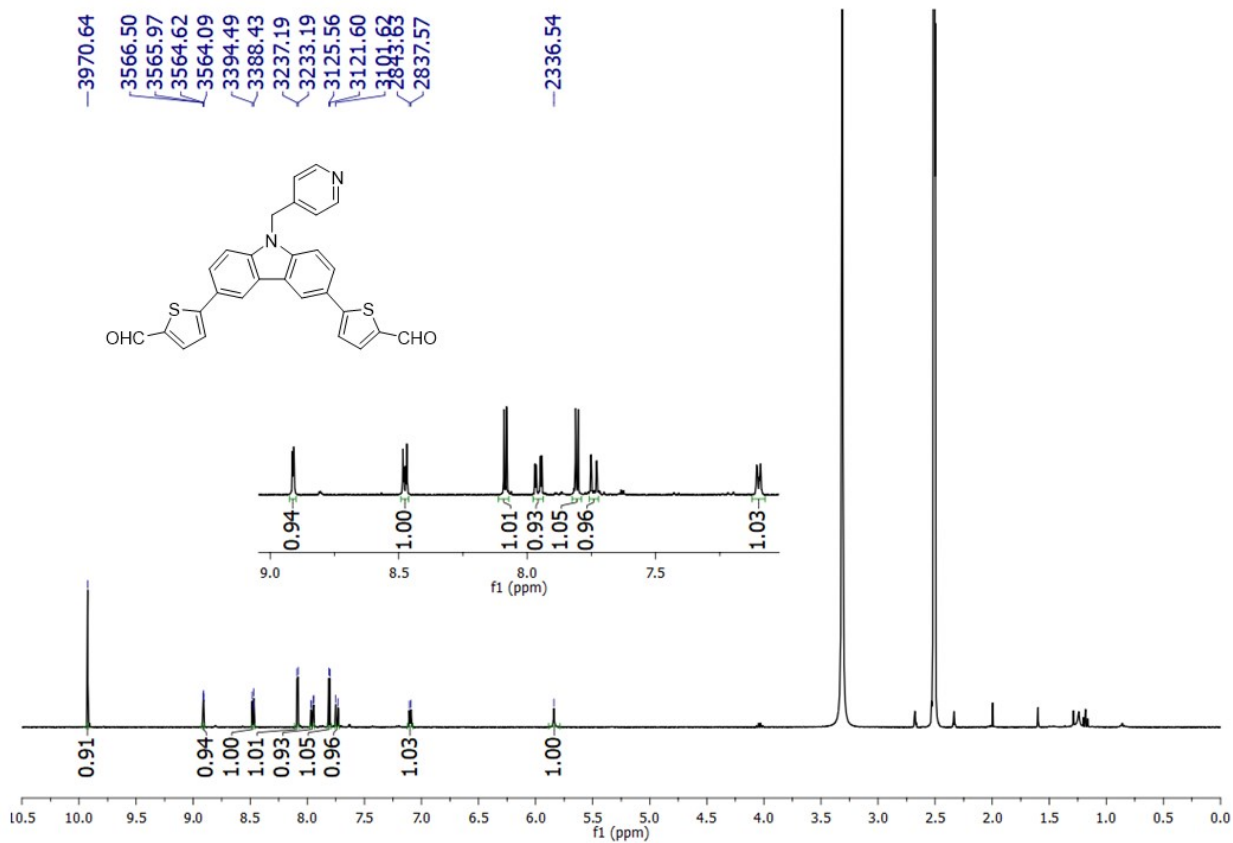


Figure S23. $^1\text{H NMR}$ of **4a** in $\text{DMSO}-d_6$.

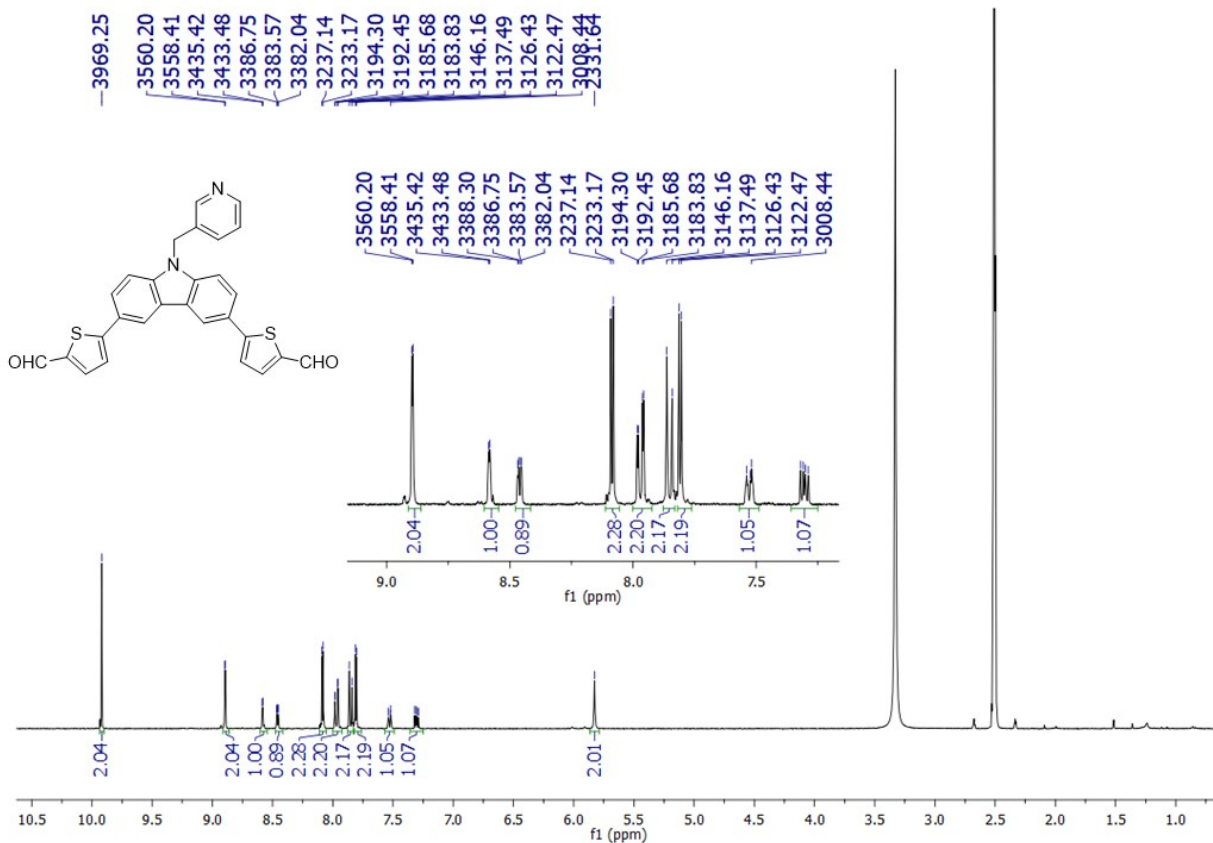


Figure S24. $^1\text{H NMR}$ of **4b** in $\text{DMSO-}d_6$.

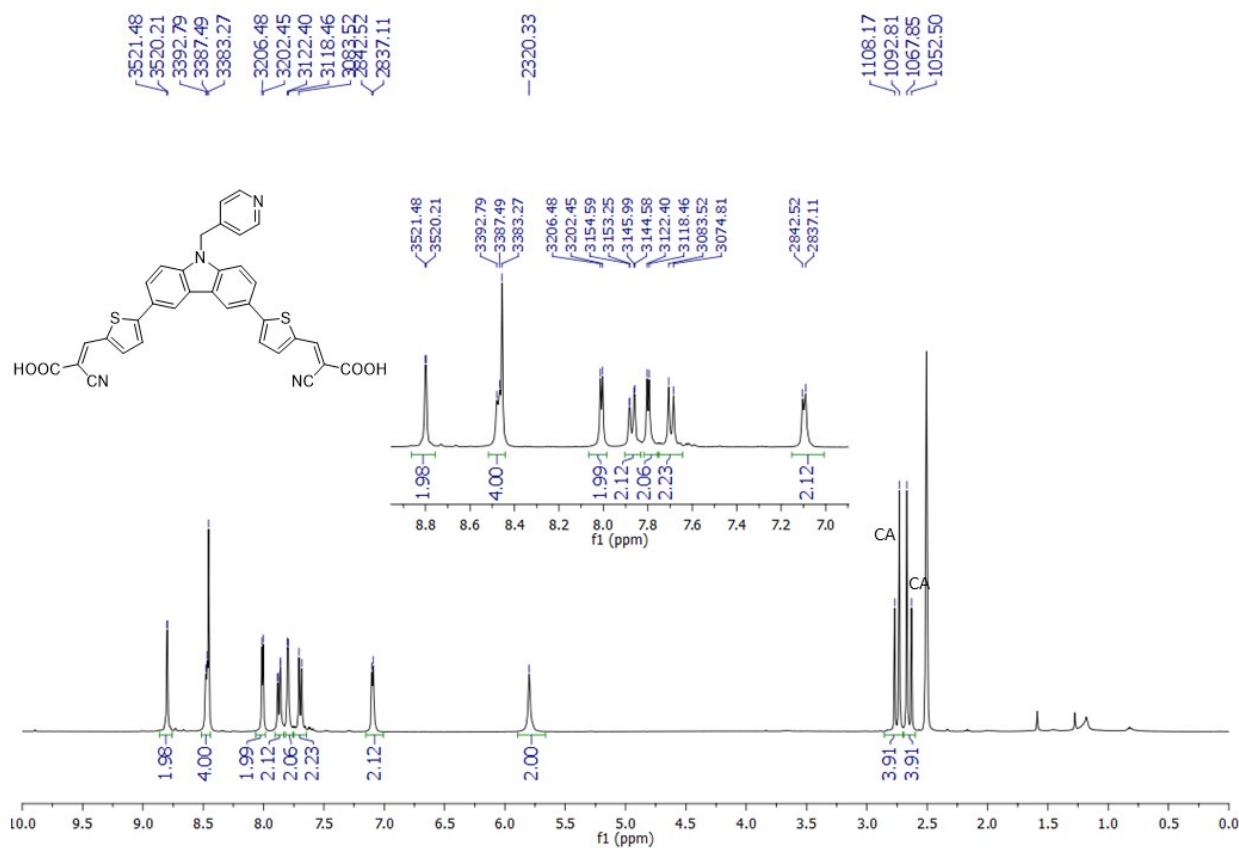


Figure S25. $^1\text{H NMR}$ of **CBZ-4Py** in $\text{DMSO-}d_6$.

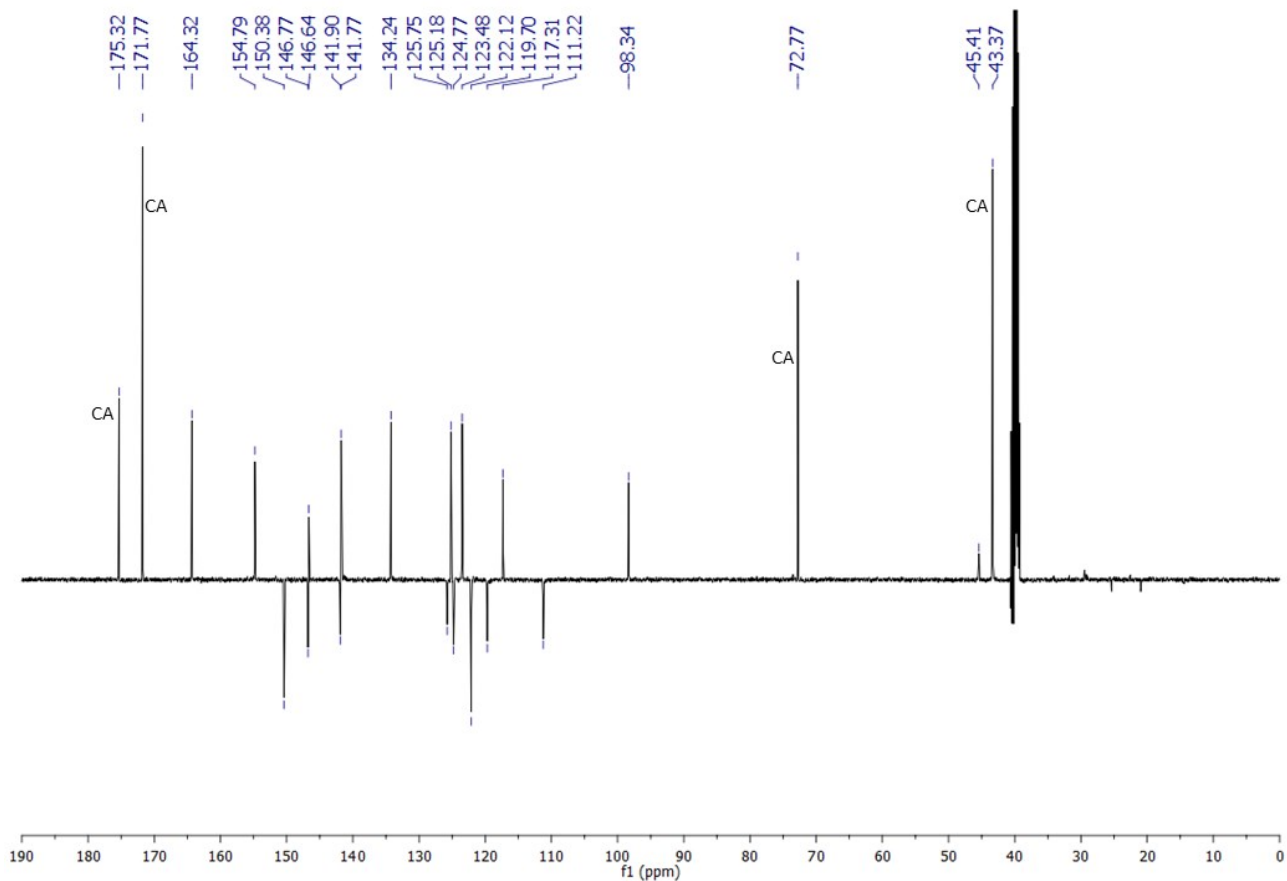


Figure S26. ^{13}C NMR of CBZ-4Py in DMSO-d_6 .

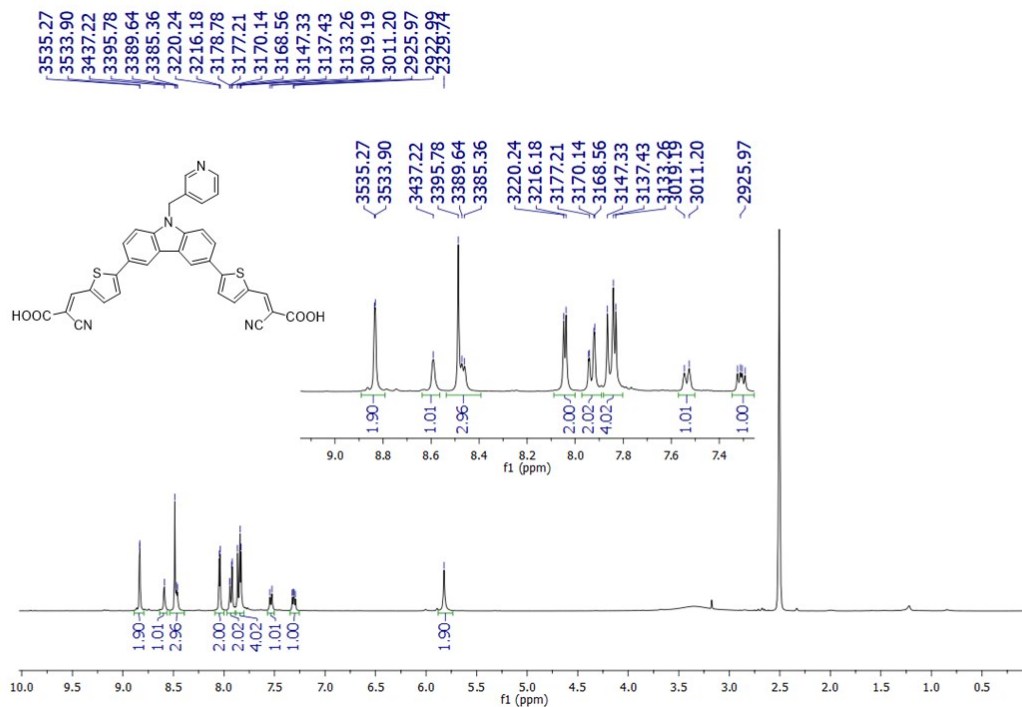


Figure S27. ^1H NMR of CBZ-3Py in DMSO-d_6 .

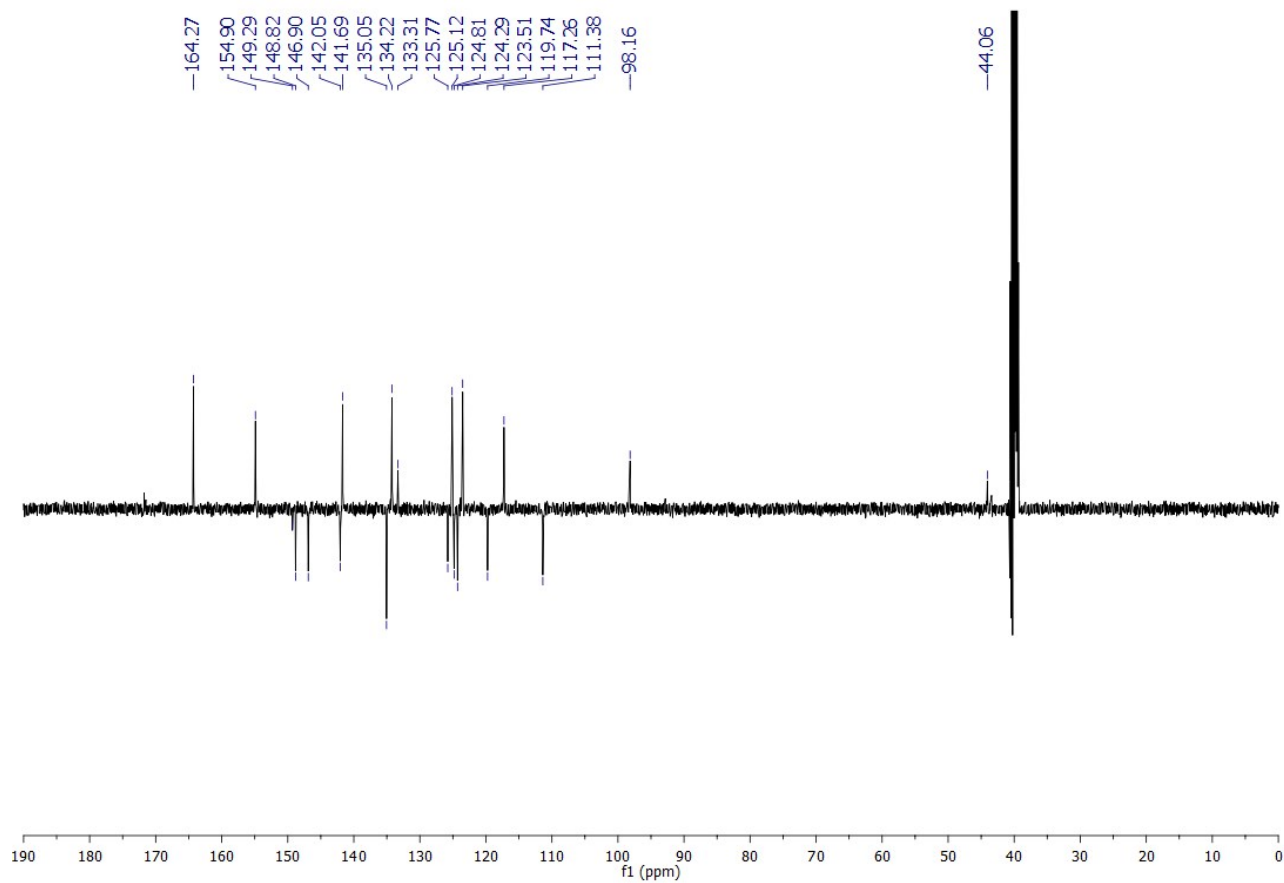


Figure S28. ^{13}C NMR of CBZ-3Py in DMSO- d_6 .

IR spectra

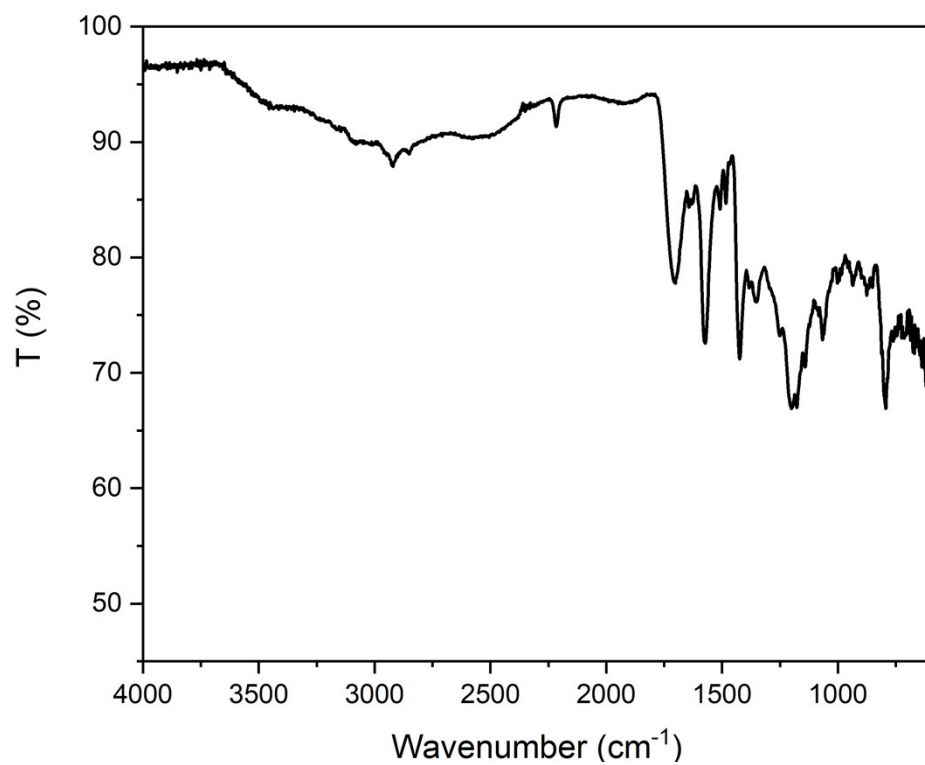


Figure S29: FT-IR spectrum of **CBZ-4Py**

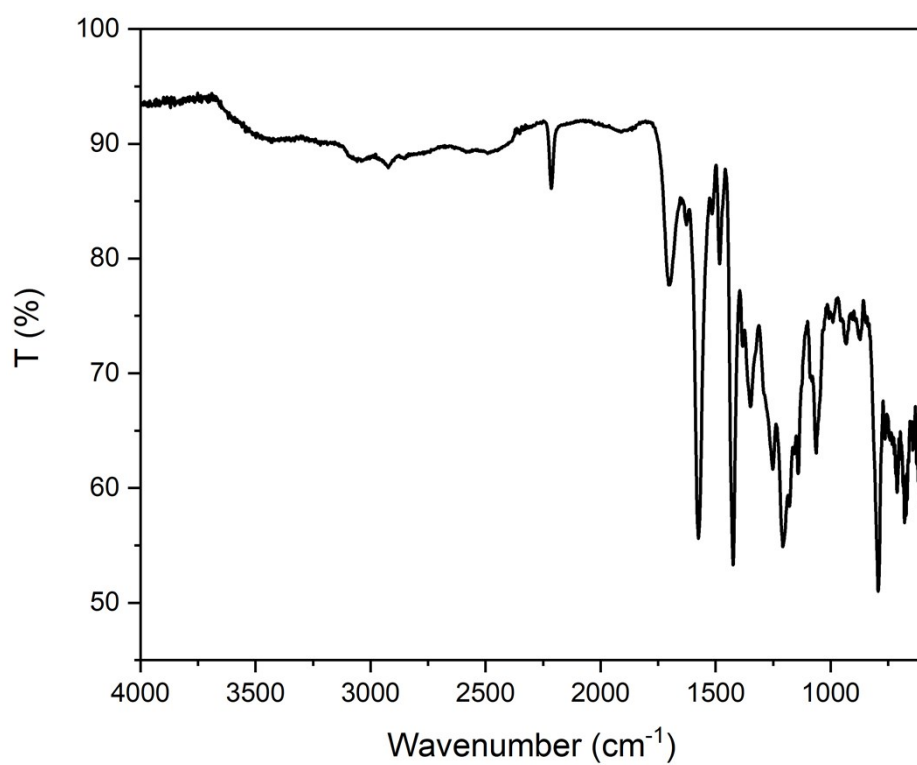


Figure S30: FT-IR spectrum of **CBZ-3Py**

HRMS spectra

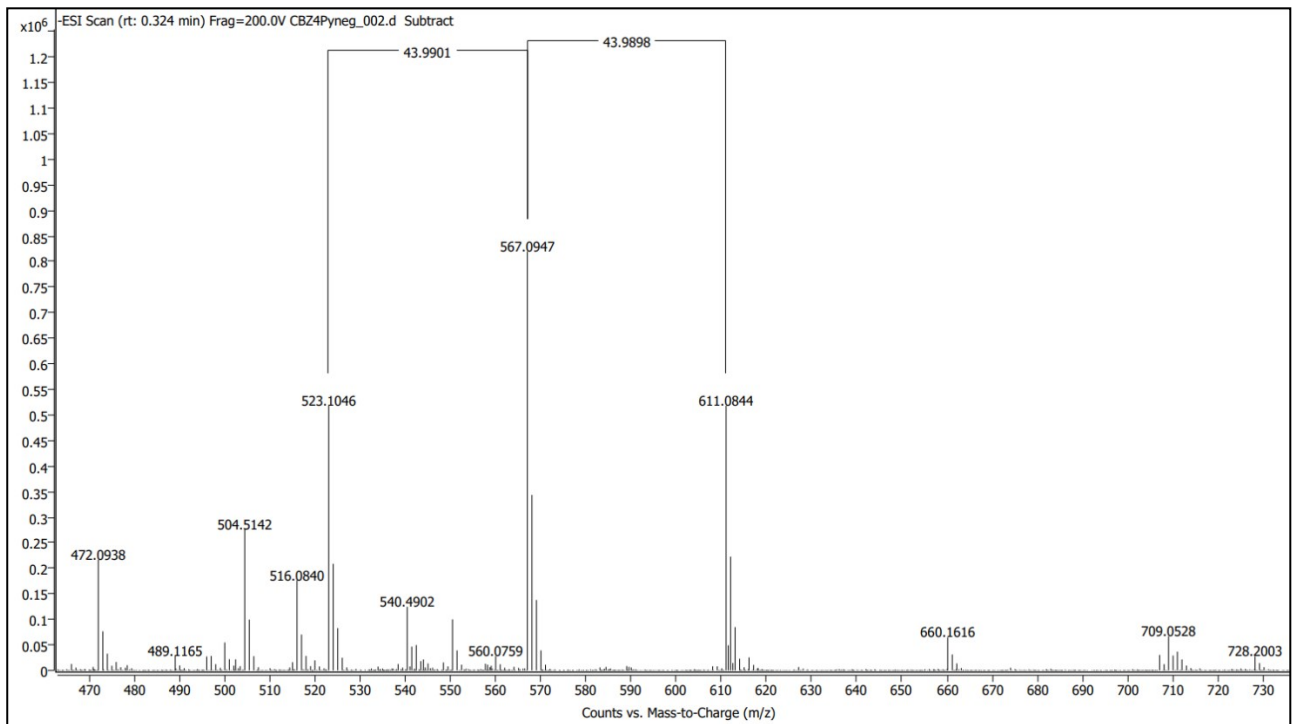


Figure S31. HRMS spectrum of **CBZ-4Py**.

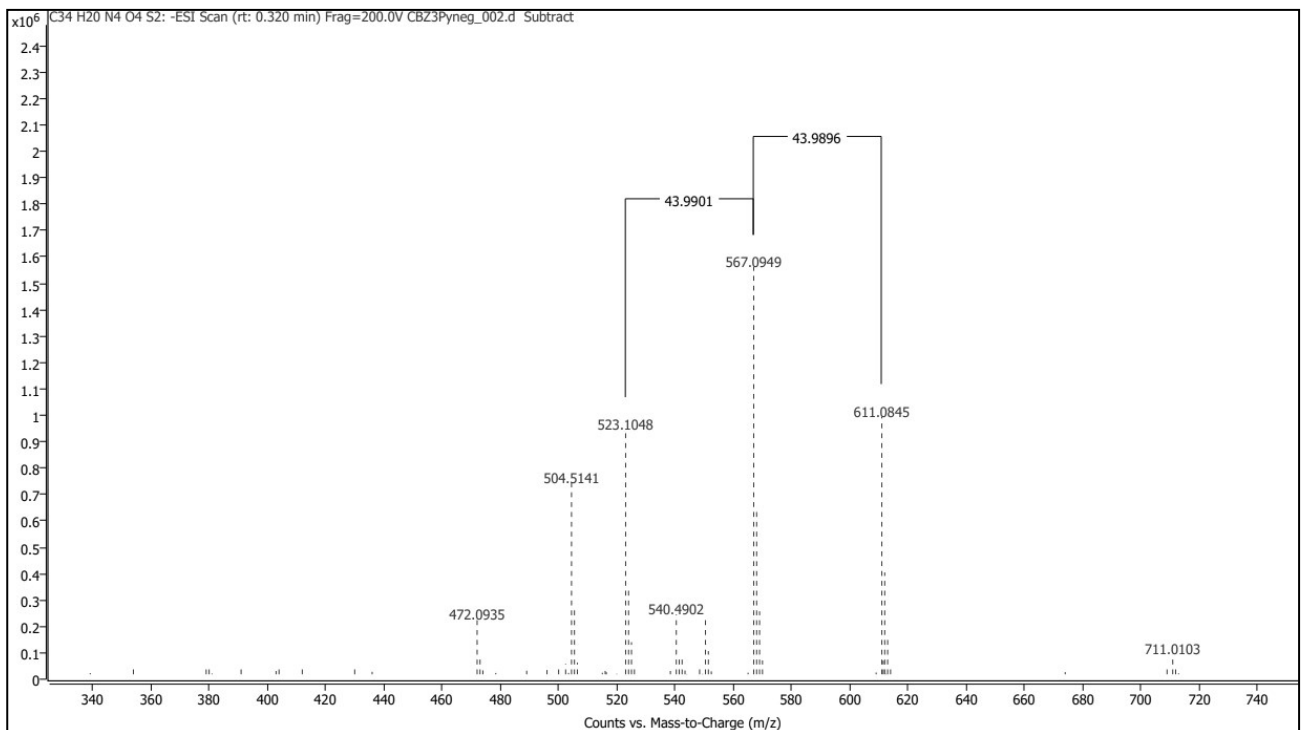


Figure S32. HRMS spectrum of **CBZ-3Py**.